Available online at www.sciencedirect.com
SCIENCE DIRECT®
Thermochimica Acta 403 (2003) 83–88
thermochimica acta
www.elsevier.com/locate/tca

Differential 3ω calorimeter

D.H. Jung [a], I.K. Moon [a], Y.H. Jeong [a,*], S.H. Lee [b]

[a] *Department of Physics, Electron Spin Science Center, Pohang University of Science and Technology, Pohang 790-784, South Korea*
[b] *Temperature–Humidity Group, Korea Research Institute of Standards and Science, Daejon 305-600, South Korea*

Received 30 November 2002; received in revised form 27 January 2003; accepted 27 January 2003

Abstract

We have developed a new dynamic calorimeter using the differential 3ω detection method. The differential 3ω calorimeter is capable of measuring dynamic heat capacity of liquid samples. The new calorimeter consists of a Wheatstone bridge made of two identical heater/sensors, and is based on the sensitive null detection method. The balancing is done automatically at all frequencies and is independent of temperature; once a sample is placed on one heater/sensor, a third harmonic signal is produced due to the difference in the two arms of the bridge. The differential 3ω calorimeter provides enhancements over traditional dynamic methods in dynamic range (up to 30 kHz), resolution, and ease of operation.

Keywords: 3ω calorimeter; Differential method; Dynamic heat capacity; Glass transition

1. Introduction

Calorimetry is unique in providing a method to directly monitor the free energy change of a given system [1]. Recently there has been growing interest in generalizing heat capacity measurements as a probe to the dynamics of condensed matter [2]. Since heat capacity can be expressed as the enthalpy fluctuation from statistical mechanics, it is easily extended to the dynamic regime within linear response theory [3].

The 3ω method, an ac modulation method using a heater as sensor (heater/sensor) simultaneously, has been widely used to study both thermal and dynamic properties of matter [4]. This method was originally discovered by Corbino long ago [5], and then utilized as a dynamic tool by Holland et al. [6]. More recently, Birge and Nagel [7] used a planar heater in applying the same method to probe the slow dynamics associated with glass transition, while Cahill et al. [8] utilized a thin line heater to measure the thermal conductivity of solids. Theoretical basis and experimental setup of this method were reviewed by various authors [2,9,10].

Since dynamic heat capacity $C_p(\omega)$ includes contributions from all degrees of freedom in matter [11], the 3ω calorimeter is an excellent tool in probing dynamic nature for a system [12]. In contrast, other tools may couple to a specific degree of freedom; for example, dielectric spectroscopy only couples to either electric charges or dipoles. Despite its value as a dynamic probe, the dynamic range of the 3ω calorimeter is limited and its sensitivity is poor compared to, for instance, dielectric spectroscopy. To enhance the dynamic range and sensitivity, the 3ω method adopting a multiband heater/sensor and a substrate with a small heat capacity times thermal conductivity·($C_p\kappa$) value were attempted [9,10].

* Corresponding author. Tel.: +82-542792078; fax: +82-542798056.
E-mail address: yhj@postech.ac.kr (Y.H. Jeong).

0040-6031/03/$ – see front matter
doi:10.1016/S0040-6031(03)00082-0

In this article we introduce a modification of this method using two identical heater/sensors. The new calorimeter, termed as differential 3ω calorimeter, consists of a Wheatstone bridge made of two identical heater/sensors, and is based on the sensitive null detection method. The balancing is done automatically at all frequencies and is independent of temperature; once a sample is placed on one heater/sensor, a third harmonic signal is produced due to the difference in the two arms of the bridge. The differential 3ω calorimeter provides enhancements over traditional dynamic methods in both dynamic range (up to 30 kHz) and resolution. The improvements made in sensitivity, wide dynamic range and stability are demonstrated for a glycerol–amine binary mixture.

2. Differential 3ω calorimeter

The Wheatstone bridge circuit adopted in the previous version of the 3ω method to measure the third harmonic signal is shown in Fig. 1a [13]. Here R_1 and R_2 are fixed resistors, while R_v is a variable one. Normally the resistors in the left arm are designed to be of the order of a few kilo-ohm, so that the majority of the current flows into the heater/sensor R_{sh}. If one drives the bridge circuit with a current at angular frequency ω, $I(t) = I_0 \cos(\omega t)$, the third harmonic voltage induced across the bridge is given by:

$$V_{3\omega} = \frac{1}{2}\left(\frac{R_1}{R_1 + R_{sh}}\right) I_0 R_{sh} \alpha |\delta T_h| \cos(3\omega t + \phi) \quad (1)$$

where ϕ represents the phase shift of the induced temperature oscillation δT_h with respect to the power oscillation. The temperature and power oscillations, of course, occur at 2ω. R_1 and R_{sh} represent the resistance, and α does the temperature coefficient of R_{sh}. For a planar heater/sensor placed on the surface of a substrate, the temperature oscillation δT_h is given by:

$$\delta T_h = \frac{P_0}{\sqrt{2\omega C_{ps} \kappa_s}} e^{-i\pi/4} \quad (2)$$

where P_0, C_{ps} and κ_s are the power per unit area of the heater, the heat capacity per unit volume, and the thermal conductivity of the substrate, respectively. (Note that heat capacity in this paper means heat capacity per unit volume throughout.) Now if a liquid sample is put on top of the heater/sensor, there would exist two different media on the opposite sides of the heater/sensor. It is then straightforward to show that Eq. (2) becomes:

$$\delta T_h = \frac{P_0}{\sqrt{2\omega C_{ps} \kappa_s} + \sqrt{2\omega C_p \kappa}} e^{-\pi/4} \quad (3)$$

where C_p and κ are the heat capacity per unit volume and the thermal conductivity of the liquid.

The modified Wheatstone bridge for the differential 3ω method is shown in Fig. 1b. The bridge consists of two identical sets of resistors, each set with a fixed resistor R and a heater/sensor R_{sh}. Both R and R_{sh} are of the order of 50 Ω. The fixed resistors are made of manganin wire with very small temperature coefficient of resistivity to suppress unnecessary third harmonic generation. Two identical heater/sensors, that is, two metal films deposited on a glass substrate, reside in an experimental stage maintaining the same temperature. Even when a sinusoidal current flows through the circuit, there would be no signal across the bridge at both the fundamental and its harmonics due to the intrinsic balancing. But as soon as a sample is placed on one of the heater/sensors, a 3ω signal appears. Since the 3ω signal is generated due to the difference in temperature oscillations from the two heat/sensors (one with a sample and one without), the third harmonic voltage

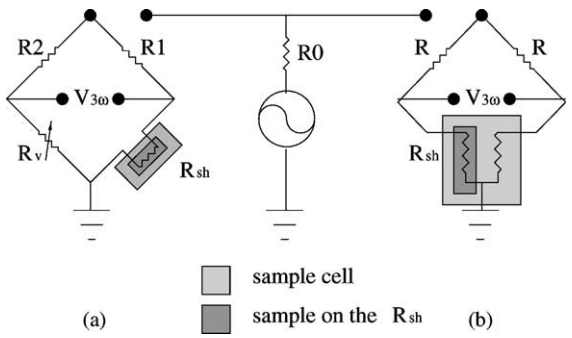

Fig. 1. Wheatstone bridge circuits for the third harmonic detection with a signal source (output impedance R_0) are shown. (a) A conventional circuit. R_1 is a resistor made of manganin wire with a small temperature coefficient of resistivity, and the resistance of R_2 and a variable resistor R_v is a few orders of magnitude larger than that of the right arm resistances. (b) A differential circuit. The bridge consists of two equivalent sets of resistors R and R_{sh}. The resistance of R and R_{sh} is about 50 Ω each. When a sample is placed on one of the R_{sh}s as designated by a dark shade, $V_{3\omega}$ due to a difference in temperature oscillations of R_{sh} is generated.

induced across the bridge is given by:

$$V_{3\omega} = \frac{1}{4}\left(\frac{R}{R+R_{sh}}\right) I_0 R_{sh}\alpha|\delta T_{hL} - \delta T_{hR}|\cos(3\omega t + \phi) \quad (4)$$

where δT_{hL} (temperature oscillation from the left arm with a sample) and δT_{hR} (from the right side without a sample) are given by Eqs. (2) and (3), respectively. ϕ is the phase shift of the complex amplitude $(\delta T_{hL} - \delta T_{hR})$ with respect to the input power oscillation. It is noted that the expression of Eqs. (2) and (3) includes $C_{ps}\kappa_s$ in the denominator, and thus the background signal from the substrate is not completely eliminated. Nevertheless, the signal becomes much more sensitive to the sample properties.

For the conventional 3ω method, one has to balance the bridge as temperature changes because the heater/sensor resistance varies, and parasitic capacitance usually induces an out-of-phase component across the bridge due to the mismatch of right and left resistors. This effect becomes severe at high frequencies and requires an additive capacitor placed across R_{sh}. In contrast, the present design with two identical heater/sensors would make bridge balancing independent of temperature and frequency by symmetry. As the temperature of the two heater/sensors is the same all the time, the balanced state is not disturbed by a temperature fluctuation. Moreover, there would be no out-of-phase signal caused by parasitic cable capacitances. In actual implementation of the differential 3ω method, however, one has to add a variable resistor R_v to one of the arms in parallel and use it for fine control. This is because the resistance and temperature coefficient of the two heater/sensors differ to minute degree, even if every effort is made to fabricate them identically. Since the difference in resistance between the two heater/sensors (approximately 50 Ω each) is less than 1%, the value of R_v needed is of the order of 50 kΩ. Before leaving this section, it is pointed out again that although a signal is detected at 3ω, temperature oscillation occurs at 2ω.

3. Sample cell

Two identical heater/sensors are obtained by thermally evaporating Ni onto a thick window glass of thickness 6 mm as illustrated in Fig. 2. Ni films are preferred as heater/sensor because they have a large temperature coefficient of resistance. The zigzag-shaped heater/sensors have the dimension of 6 mm × 6 mm, and the distance between them is 6 mm. To protect the heater/sensors from chemical or electrical problems, SiO_2 of thickness ∼2000 Å is deposited on top of the heater/sensors. The two heater/sensors have to be separated by a few times the thermal diffusion length at the lowest measuring frequency, $\lambda_T = \sqrt{\kappa_s/2\omega C_{ps}}$, in order to be free from an interference between the two heater/sensors. As the diffusion length of the window glass at 10^{-2} Hz is approximately 2 mm, we chose the separation distance to be 6 mm. During the course of experiment, it is important to make the vacuum level remain stable at a low value (less than 10^{-4} Torr); otherwise the heater/sensor of the reference side measures not only the thermal property of the substrate but also that of air. Careful attention should be paid to the contacts which connect lead wires to the heater/sensors. The lead contacts can be considered to consist of contact resistance and capacitance in parallel, and they may give rise to contamination in phase and amplitude of the third harmonic signal.

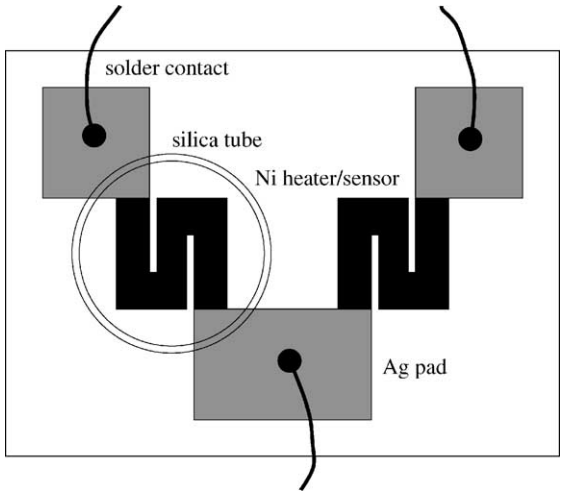

Fig. 2. A schematic diagram of the sample cell. Two equivalent R_{sh}s and lead pads are deposited on a window glass of thickness 6 mm. Zigzag-patterned Ni film resistors are used to obtain a reasonable value of resistance. The dimension of R_{sh} is 6 mm × 6 mm, and the distance between the two heater/sensors is also 6 mm. The lead pads of thickness 1 μm are made of Ag deposited on the Ni films. On top of one of R_{sh}s, a silica tube of height 10 mm is placed to contain a liquid sample.

4. Experimental results and discussion

In order to study the correlation between atomic scale short range order and macroscopic structural relaxation of supercooled liquids, we have measured the dynamic heat capacity of binary mixtures, $(\text{glycerol})_x(\text{1,3-propanediamine})_{1-x}$ using the differential 3ω calorimeter. Here we present only the data for the $x = 0.4$ case to demonstrate the characteristic features of the present method, and leave discussions on the whole data to future publications [14].

Fig. 3 shows the frequency dependence of the third harmonic signal at room temperature, for a fixed current of $I_0 = 17\,\text{mA}$, covering more than six decades. Although we measured differential $V_{3\omega}$, the amplitude of the signal should follow $1/\sqrt{\omega}$ and the phase be constant at $-\pi/4$ as a function of frequency for a planar heater/sensor. A deviation of measured $V_{3\omega}$, represented by circles in the plot, from the theoretical behavior is evident below 1 Hz. This deviation is caused by the finite size effect of the heater/sensor, and can be corrected.

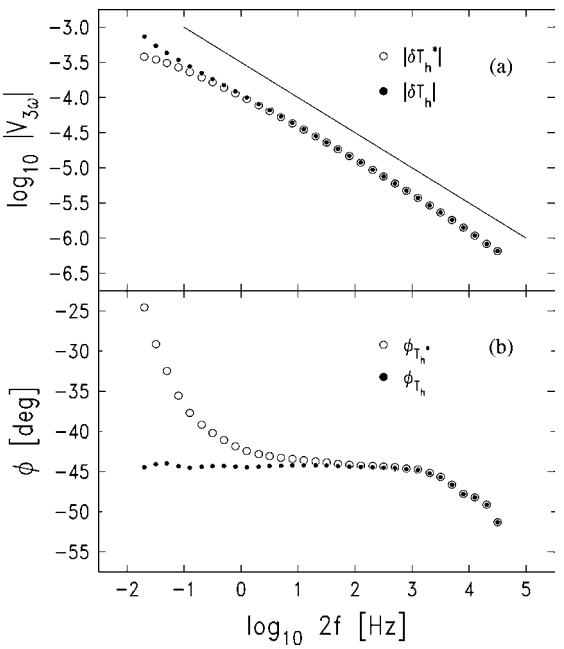

Fig. 3. The frequency dependence of $V_{3\omega}$, measured by the differential 3ω method, from $(\text{glycerol})_{0.4}(\text{1,3-propanediamine})_{0.6}$ at room temperature: (a) signal amplitude, and (b) phase. $2f$ is the frequency of temperature oscillation. The solid line in (a) with slope $-1/2$ is a guide to the eye. The open circles represent the measured data points, while the black dots do the corrected values.

Note that temperature oscillations given in Eqs. (2) and (3) are the solution to the ideal one-dimensional problem, and the measured signal would deviate from the ideal case as the finite heater/sensor width becomes comparable to the thermal diffusion length. Then, the expression for the measured signal should include δT_h^*, real temperature oscillation, instead of the original δT_h for the ideal situation. The relationship between these two was already derived by Birge et al. [9,15] as:

$$\delta T_\text{h}^* \simeq \text{e}^{\text{i}\varphi}(1-\varphi)\delta T_\text{h} \tag{5}$$

where φ is a dimensionless parameter representing the finite size effect. For a planar heater/sensor of width W placed on the surface of a substrate, φ is given by:

$$\varphi = \frac{\lambda_\text{T}}{W} = \frac{1}{W}\sqrt{\frac{\kappa_\text{s}}{2\omega C_\text{ps}}} \tag{6}$$

When a liquid is placed on the substrate, Eq. (6) is generalized in a straightforward manner,

$$\varphi = \frac{1}{W}\left|\frac{\kappa_\text{s}+\kappa}{\sqrt{2\omega C_\text{ps}\kappa_\text{s}}+\sqrt{2\omega C_\text{p}\kappa}}\right| \tag{7}$$

This finite size effect should clearly manifest itself around the glass transition. As a glass-forming liquid goes through the glass transition, the heat capacity takes the value of a liquid above the glass transition and that of a solid below. As a result, a step-like change in the measured phase in association with a amplitude change is expected.

In Fig. 4 plotted are the amplitude and phase of the temperature oscillation at $2f = 0.08\,\text{Hz}$, as measured by the differential 3ω method, in the vicinity of the glass transition of a binary mixture $(\text{glycerol})_{0.4}(\text{1,3-propanediamine})_{0.6}$. Fig 4a displays an amplitude variation of the measured temperature oscillation δT_h^* as a function of temperature. An abrupt change in heat capacity C_p through the glass transition gives rise to a corresponding change in amplitude, because κ·remains nearly constant as the system undergoes the transition [13]. Fig. 4b is a plot of the measured phase as a function of temperature. First of all, a peak in the phase is seen; the peak is caused by the imaginary part of heat capacity, a typical feature of relaxation associated with the glass

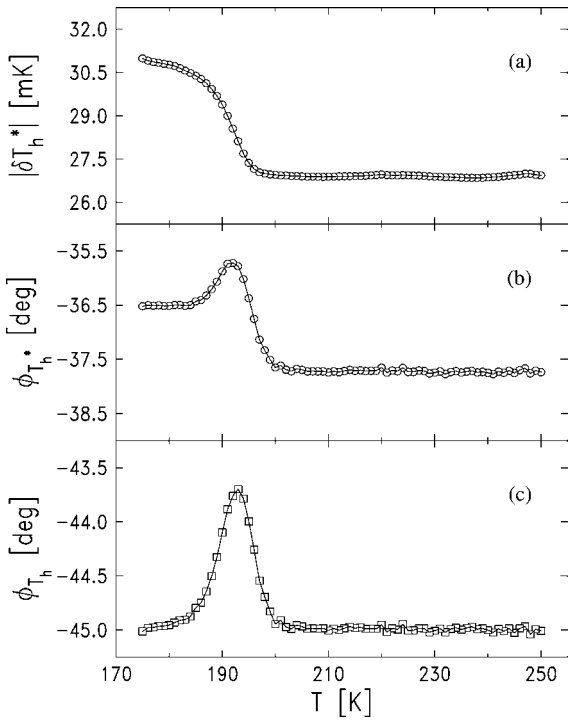

Fig. 4. The finite size effect near the glass transition of the glycerol–amine mixture. Measurements were done at $2f = 0.08$ Hz. (a) Glass transition is easily seen from a variation in the amplitude of δT_h^* as a function of temperature. (b) The peak in the phase is due to the glass transition. It should be noted that the baseline value of the phase deviates from -45°, and shows a step-like change before and after transition, and these are caused by the finite size effect. (c) The base line value of the phase corrected for the finite size effect is -45°, as the one-dimensional heat diffusion equation would predict.

transition. It should be noted that the baseline value of the phase deviates from -45°, and shows a step-like change before and after transition. These behaviors are caused by the finite size effect. Using the relation between $|\delta T_h^*|$ and $|\delta T_h|$ in Eq. (5), one can easily calibrate δT_h^*. The calibrated phase δT_h is shown in Fig. 4c, and its baseline takes -45 degrees above and below the glass transition. Similarly, if we take the finite size effect into account and correct the data using the relationship between δT_h and δT_h^*, both the amplitude and phase of the measured differential signal follow the ideal expression as displayed in Fig. 3 (black dots).

Now turning to the high frequency part of Fig. 3, it is seen that a deviation from the ideal behavior occurs above a few kilohertz, particularly in the phase. What is the cause of this deviation at high frequencies? Although we do not have a complete understanding at present, one possibility may be that the deviation is caused by a confinement of temperature oscillation only to the heater/sensor at high frequencies. Since the thermal diffusion length for a typical insulator becomes a few micrometers above, say, 10 kHz, the mass ratio of a liquid sample within the thermal diffusion length to the heater/sensor including the SiO_2 layer becomes only a few percent. Considering the fact that if temperature oscillation is confined only to the heater/sensor, the phase shift should go to -90°, the deviation at high frequencies may be explicable. Since this confinement effect naturally arises at high frequencies with a decrease in thermal diffusion length, it does not seem to be possible to avoid it. Nevertheless, by taking the value of phase at room temperature as reference and measuring relative deviations, the dynamic range was extended to 30 kHz. In fact, it appears to be possible to extend the method close to 100 kHz, if one adopts a thinner film for the heater/sensor than the ones used in the present experiment and also eliminates the oxide layer. Extending the working frequency range up to 100 kHz means that one would be able to measure thermophysical properties of films of thickness sub-microns, and therefore is well worth pursuing in view of the proliferation of nanotechnology.

It should also be emphasized that the differential method enhances S/N ratio particularly at high frequencies. It is now possible to detect changes as small as a few parts in 10^{-4} in amplitude and 0.01 degree in phase. In Fig. 5 we show a whole data set of complex $C_p\kappa = (C_p\kappa)' - i(C_p\kappa)''$ of the binary mixture $(\text{glycerol})_{0.4}(\text{1,3-propanediamine})_{0.6}$ versus $\log_{10} 2f$ at various temperatures; the quality of the data is evident. As is seen from the data the system shows a typical glassy behavior, that is, the dynamics of the system slows down with decreasing temperature and the shape of $(C_p\kappa)''$ is asymmetrical. It may be noted that this relaxational behavior (or frequency dependence) of the directly measured quantity, complex $C_p\kappa$, is mainly due to complex heat capacity, $C_p(\omega)$, because κ remains frequency-independent in the supercooled region [13]. In many glass formers in the literature [16], glassy relaxational behaviors are described well with a Fourier transform of the Kohlrausch–Williams–Watts

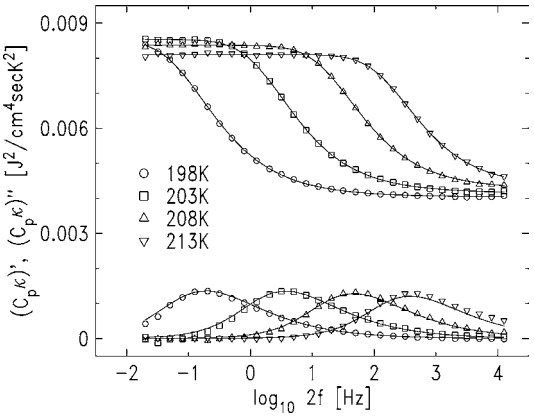

Fig. 5. $(C_p\kappa)'$ (top) and $(C_p\kappa)''$ (bottom) of $(\text{glycerol})_{0.4}$(1,3-propanediamine)$_{0.6}$ as a function of frequency at various temperatures. The data were taken by the differential 3ω method. The symbols denote the data points, and the solid lines are fits to the data with the Kohlrausch–Williams–Watts function, $\exp[-(t/\tau)^{\beta}]$, with $\beta = 0.56$ (198 K), 0.57 (203 K), 0.58 (208 K), and 0.59 (213 K).

function, $R(t) = \exp[-(t/\tau)^{\beta}]$. The solid lines in the figure represents the fitting results with excellent coincidence with the experimental data.

In conclusion, we have developed a new dynamic calorimeter using the differential 3ω detection method. The differential 3ω calorimeter is capable of measuring dynamic heat capacity and thermal conductivity of solid or liquid samples with wide dynamic range (up to 30 kHz), high sensitivity (a few parts in 10^{-4} in amplitude and 0.01° in phase), and ease of operation.

This work was supported by the SRC program of KOSEF and the fund from KRISS.

References

[1] B. Wunderlich, Thermal Analysis, Academic Press, San Diego, 1990.
[2] Y.H. Jeong, Thermochim. Acta 304–305 (1997) 67.
[3] R. Kubo, Rep. Prog. Phys. 29 (1966) 255.
[4] Y. Kraftmakher, Phys. Rep. 356 (2002) 1.
[5] O.M. Corbino, Physica Z 12 (1911) 292.
[6] L.R. Holland, J. Appl. Phys. 34 (1963) 2350; L.R. Holland, R.C. Smith, Abid 37 (1966) 4528.
[7] N.O. Birge, S.R. Nagel, Rev. Sci. Instrum. 58 (1987) 1464.
[8] D.G. Cahill, H.E. Fisher, T. Klitsner, E.T. Swartz, R.O. Pohl, J. Vac. Sci. Technol. A 7 (1989) 1259.
[9] N.O. Birge, P.K. Dixon, N. Menon, Thermochim. Acta 304–305 (1997) 51.
[10] J. Korus, M. Beiner, K. Busse, S. Kahle, R. Unger, E. Donth, Thermochim. Acta 304–305 (1997) 99.
[11] T. Christensen, J. Phys. (Paris) 46 (1985) C8-635.
[12] D.H. Jung, T.W. Kwon, D.J. Bae, I.K. Moon, Y.H. Jeong, Meas. Sci. Technol. 3 (1992) 472.
[13] I.K. Moon, Y.H. Jeong, Rev. Sci. Instrum. 67 (1996) 29.
[14] D.H. Jung, Y.H. Jeong, unpublished.
[15] H.S. Carsaw, J.C. Jaeger, Conduction of Heat in Solids, Clarendon Press, New York, 1959.
[16] K.L. Ngai, E. Riande, G.B. Wright (Eds.), J. Non-Cryst. Solids 172–174 (1994).